JOURNAL OF THERMOPHYSICS AND HEAT TRANSFER
Vol. 13, No. 2, April–June 1999

Geometric Optics Applied to Rough Surfaces Coated with an Absorbing Thin Film

Kakuen Tang,* Paul A. Kawka,† and Richard O. Buckius‡
University of Illinois at Urbana–Champaign, Urbana, Illinois 61801

The geometric optics approximation in which the interference effects are neglected has been shown to accurately predict surface reflection from random rough surfaces over a large domain of geometric parameters. In this work, the geometric optics approximation is extended to rough surfaces coated with an absorbing thin film. Multiple reflections and the effects of interference within the thin film are considered. The thin film model predictions are compared with the experimental findings for an aluminum surface coated with a thin aluminum-oxide composite film. Such comparisons made at a variety of incident angles and wavelengths indicate that the geometric optics thin film model is accurate. The approximate solutions also indicate that a significant amount of energy is absorbed by the thin film, leading to a decrease in the reflected energy. The model is used to demonstrate the strong influence of optical constants and film thickness on the reflection distribution.

Nomenclature

h = film thickness
n = surface refractive index
r = amplitude of the reflected wave
x, y, z = surface coordinates
β = phase angle
θ = polar angle
κ = absorption index
λ = wavelength
ρ'', ρ' = bidirectional reflectivity, directional reflectivity
σ = surface height deviation
τ = surface correlation length
Φ = radiant power flow
ϕ = azimuthal angle
Ω = solid angle

Subscripts
m, l = indices
s = scattered
0 = incident
1, 2, 3 = medium

Superscript
$''$ = bidirectional

Introduction

ELECTROMAGNETIC theory[1,2] provides exact solutions for wave scattering from interfaces. The solutions are dependent on incident direction θ_0, ϕ_0; incident wavelength λ; optical constants $n - i\kappa$; and surface geometric parameters, including correlation length τ and surface height deviation σ. Electromagnetic theory approaches are derived from Maxwell's equations and involve multiple coupled integral equations. In general, these approaches require a significant amount of computational memory and time units.

Received Sept. 22, 1998; revision received Dec. 3, 1998; accepted for publication Dec. 7, 1998.

*Currently, Staff Engineer, Hughes Space and Communications Company, M/S D562, P.O. Box 92919, Los Angeles, CA 90009-2919.

†Graduate Student, Department of Mechanical and Industrial Engineering.

‡Professor and Head, Department of Mechanical and Industrial Engineering. Associate Fellow AIAA.

Because of the complexity of electromagnetic theory, various approximate solutions have been developed for wave scattering from random rough surfaces. The Fresnel[3,4] and Lambertian models[5,6] are two frequently used approximations. The Fresnel approximation assumes specular reflection, and all energy is reflected within the solid angle cone surrounding the specular angle. In the Lambertian model, energy is assumed to be equally distributed through the entire hemisphere so that the bidirectional reflectivity is simply the cosine of the scattering angle multiplied by a weight factor. The Kirchhoff approximation,[4,7–11] unlike the Fresnel and Lambertian approximations, can predict the reflection distribution between specular and diffuse. At every surface node, the scattered magnetic and electric fields are approximated by the field that would exist on a tangent plane to the surface at this point. The domain of validity has been constructed, and the Kirchhoff approximation can predict an accurate solution when the surface length scales σ and τ are comparable with the incident wavelength λ. In addition, the surface slope σ/τ must be less than 0.3.

Tang et al.[12] and Tang and Buckius[13] studied the geometric optics approximation in which energy bundles incident on a surface are traced through multiple interactions until the bundles leave the surface. Comparisons of approximate solutions using geometric optics were made to calculations based on electromagnetic theory and to existing experimental findings, and it has been proven that this approximation can predict specular, diffuse, and retroreflection (energy reflected back in the incident direction) for random rough surfaces. In addition, the geometric optics approximation can provide an accurate solution for surfaces with a slope σ/τ as large as 4.0.

Research has been performed on reflection from thin film surfaces because of applications in spectroscopic instruments, in optical property measurements, in surface contamination, in semiconductor devices, etc. Most of the investigations focus on flat surfaces with only a few cases of slightly rough and deterministic or patterned surfaces. The effects of the outgassing product film on flat optical surfaces were determined.[14,15] In that program, contamination potential for often-used satellite materials including adhesives, paints, and lubricants were studied. Nguyen and Rustgi[16] used the Rayleigh method to study the reflection from multilayered surfaces that consist of layers of flat thin dielectric film on one-dimensional sinusoidal metallic surfaces with surface slopes around 0.02. Gunde and Aleksandrov[17] calculated the infrared optical constants for a silicon-oxide film deposited on the Czonchralski-grown silicon

wafer based on the measured reflectance and transmittance. A reflection model[3,18] for flat surfaces incorporating roughness factors[19] was used in these investigations. Similar studies[20-22] were conducted on various thin film materials on a slightly rough surface.

This work addresses reflection distribution from two-dimensional metallic and perfectly conducting rough surfaces coated with an absorbing thin film. The surface length scales are on the order of, or less than, the incident wavelength. The geometric optics approximation is extended to calculate the bidirectional reflectivity for thin film surfaces. The primary goals for this study are to quantify the accuracy of the approximation and to analyze the influence of optical constants and film thickness on reflection distribution. The next section presents the analysis, including the radiative property definition, the surface prescription, and the thin film geometric optics approximation. The experimental system and the surface sample are then discussed. The predictions based on this model are compared with experimental findings in the Results and Discussion section.

Analysis

Radiative Properties

The bidirectional reflectivity is used to quantify the reflection distribution and is defined as π times the ratio of the reflected power per unit solid angle per unit projected area to the total incident power.[3] The bidirectional reflectivity is given as

$$\rho''_\lambda(\Omega_0, \Omega_s) = \frac{\pi \dfrac{d\Phi_s}{d\Omega_s}}{\cos(\theta_s)\dfrac{d\Phi_0}{d\Omega_0}} \tag{1}$$

where Φ and Ω are the radiant power and solid angle, respectively, and the subscripts 0 and s denote incident and scattering, respectively (see Fig. 1a). The bidirectional reflectivity is the most fundamental physical quantity in radiative heat transfer and is often used to evaluate other properties. For example, integrating the bidirectional reflectivity over the entire hemisphere yields the hemispherical reflectivity,

$$\rho'_\lambda(\Omega_0) = \frac{1}{\pi}\int_{2\pi} \rho''_\lambda(\Omega_0, \Omega_s)\cos(\theta_s)\, d\Omega_s \tag{2}$$

and system emissivity can be found by subtracting the hemispherical reflectivity from one.

Random Rough Surfaces

The present study considers two-dimensional random rough surfaces that are coated with an absorbing thin film. The substrate is perfectly conducting and is assumed to be coated with an absorbing uniform thin film of thickness h and optical constants of n_2 and κ_2. The stationary stochastic process with both a zero mean and a Gaussian probability density function of the surface height is used to generate surface profiles based on the prescribed geometric parameters. In addition, this work focuses on isotropic surfaces that exhibit no preferential roughness direction. Thus, the correlation lengths in x and y dimensions are set equal and are denoted by τ.

Thin Film Geometric Optics Approximation

A detailed geometric optics analysis for one-dimensional and two-dimensional random rough surfaces has been reported in Refs. 12 and 13, and the thin film analysis of a flat plate is discussed in Ref. 3. Thus, the description provided in this section is brief. The geometric optics approximation to electromagnetic theory is a ray-tracing approach that provides a multiple scattering solution for surface reflection. In the approximation, a random rough surface profile is first generated along with the surface slopes for each node. The angle of the incident energy bundle and the first reflection point are selected. Then the energy incident is traced through multiple interactions with the surface until it leaves the surface and contributes to the reflection distribution. The effects of interference are neglected. This assumption is valid because the random rough nature of these surfaces creates no coherent interference patterns. Fresnel reflection is applied to each local point of intersection to estimate the fraction of reflected energy, and the shadowing effects are also considered. The same scattering process is repeated for different first reflection positions with the same incident angle. A statistically accurate solution can be obtained by averaging the results over a significant number of surfaces.

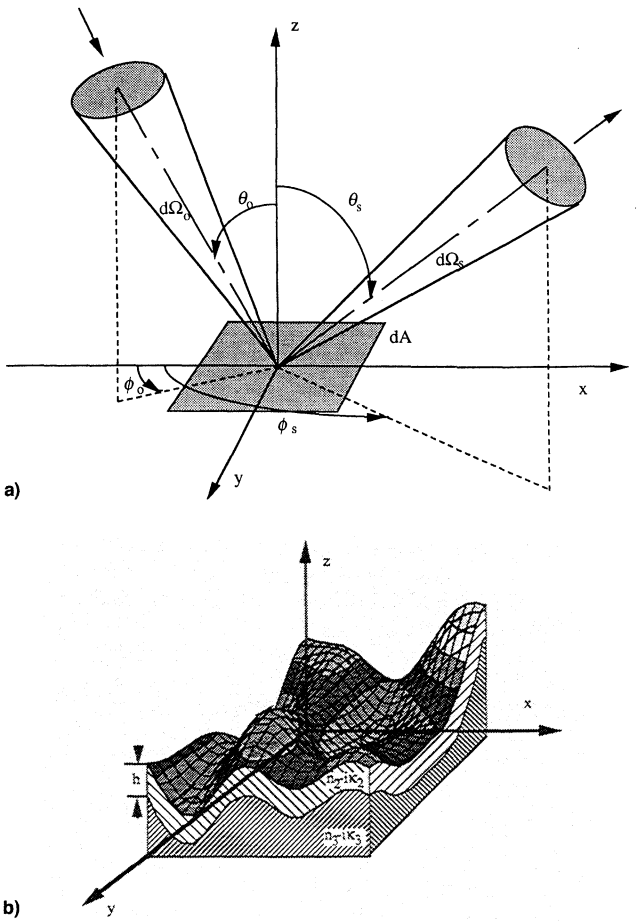

Fig. 1 Bidirectional reflection from a surface: a) notation and b) schematic of the surface cross section.

For the thin film analysis, consider an energy bundle incident upon a flat surface coated with an absorbing thin film, as shown in Fig. 1b. Two aspects need to be addressed to determine the total reflected energy: multiple reflection and interference. When a wave strikes the top surface of the thin film, some of the energy is reflected and some is transmitted through the film. Likewise, when the transmitted energy hits the bottom interface of the film, some energy is reflected and some is transmitted to the substrate. The interaction of the wave with each interface is repeated each time the wave hits an interface. Interference incorporates the phase difference between all waves reflected from the top interface of the thin film. Thus, the total reflected energy cannot be found by simply adding the energy of each wave, and multiple interface interactions must be included. The amplitude of the wave reflected from the thin film is then[3]

$$r_{\text{Film}} = \frac{r_{12} + r_{23}e^{-i2\beta}}{1 + r_{12}r_{23}e^{-i2\beta}} \tag{3}$$

where r_{ml} is the Fresnel coefficient and the subscripts m and l indicate that the energy bundles travel from medium m to medium l. Fresnel coefficients are complex numbers and are a function of the optical constants of both mediums. β is also a complex number in which the real part represents the change in phase angles that occurs as the wave passes through the thin film, and the imaginary part is proportional to the attenuation of the wave amplitude. The expression for β is

$$\beta = 2\pi n_2 h \cos(\theta_2)/\lambda \tag{4}$$

β is a function of optical constants n_2 as well as the thickness of the thin film h. The bidirectional reflectivity of the thin film flat surface can be found by squaring the magnitude of the wave amplitude ratio as

$$\rho''_\lambda = |r_{\text{Film}}|^2 \tag{5}$$

In this work, the geometric optics approximation is extended to random rough surfaces coated with a thin film that has a thickness on the order of, or less than, the incident wavelength. The scattering process is the same and the thin film is incorporated at each surface interaction. The fraction of reflected energy is calculated by Eqs. (3–5), rather than by Fresnel relations. Although the film thickness of actual surfaces varies from point to point, the thickness is assumed uniform in this geometric optics analysis to reduce the CPU time.

To yield statistically accurate results, approximately 60 realizations are required. In addition, the surface length must be at least 50λ and at least 10,000 surface nodes are necessary. The numerical error of the results presented in this work, which is dependent on the number of incident bundles, nodes, and realizations, is less than 5%. A more detailed examination of numerical errors can be found in Ref. 13. The entire numerical implementation takes about 3.5 h of CPU and 20 Mwords of memory on the Origin2000 to predict the averaged reflection distribution of 60 realizations for an intermediate rough surface with a surface slope of $\sigma/\tau = 0.36$.

Experimental Facility and Surface Samples

Reflection measurements have been conducted by utilizing a Fourier transform infrared (FTIR) spectroscopy system,[23,24] which consists of an air-cooled Ever™ source operating at 1500 K, a Michelson interferometer with a KBr splitter, a reflectometer, and a liquid-nitrogen cooled mercury cadmium telluride quantum detector. Surface samples are placed inside the reflectometer where plane and ellipsoidal mirrors, apertures, and polarizers are installed to provide control over incident and reflected angles, incident and reflected solid angles, and polarizations. Overall, this system has a capability for reflection and transmission measurements over a spectral range of 1.5–15 μm, and incident and reflected angles from 15 to 60 deg. The incident and reflected solid angles are set equal to ± 3 deg in this work.

The bidirectional reflectivity is found by the relative method.[23–25] In this method, the FTIR voltage signals are recorded for a reference standard at the calibration wavelength in which the reflection distribution is known. Then, the FTIR voltage signals are measured for the sample at the wavelength of interest, and the bidirectional reflectivity of the sample is proportional to the ratio of the voltage signals and the spectral factor. The spectral factor is determined by using an aluminum mirror, which exhibits negligible reflectivity variation over the infrared region. Desirable references have a repeatable bidirectional reflectivity with long-term stability, and they exhibit a reflection distribution that is relatively independent of incident and reflected directions. Spectralon is known to have a relatively uniform distribution in the infrared region and is selected as a reference for the FTIR measurements in this work. Its bidirectional reflectivity was performed by TMA, Inc.§ at a calibration wavelength of 3.39 μm. The overall uncertainty of the measurements is less than 10%, and a detailed discussion of the uncertainties in this FTIR system is found in Ref. 23.

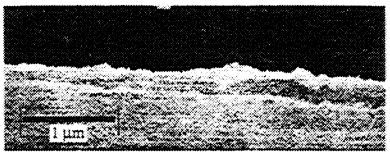

Fig. 2 SEM photograph of the cross section of the aluminum-oxide composite thin film on a flat substrate.

Reflection measurements are conducted for a two-dimensional aluminum surface coated with a layer of aluminum-oxide composite. The sample was obtained from Labsphere and was one of the random rough aluminum substrates used in their coated diffuse samples. The oxide layer was formed solely from the treatments done in their manufacturing process. To compare the experimental findings with the geometric optics thin film calculations, the optical constants and geometric parameters, as well as the thickness of the thin film are required. Similarly, measurements of the correlation length and deviation were performed by using a DEKTAK^{3}ST surface profilemeter. The measured surface slope is $\sigma/\tau = 0.36$, and the normalized deviation length is $\sigma/\lambda = 7.20$ (at an incident wavelength of 3.39 μm).

The optical constants of the aluminum substrate can be found in Ref. 3. At $\lambda = 3.39$ μm, $n_3 = 5.20$, and $\kappa_3 = 34.2$; and at $\lambda = 12.0$ μm, $n_3 = 33$, and $\kappa_3 = 103$. However, the composition of the oxide layer is uncertain; therefore, the optical constants and the thickness of the thin film coating on the random rough surfaces are determined by measuring the hemispherical reflectivity of a flat surface (the reverse side of the sample), which has been manufactured by the same process as the random rough aluminum surface. Because both the random rough and flat surface have received the same manufacturing treatment, the composition and the thickness of the oxide layers are taken to be similar. In addition, because the flat surface exhibits a specular reflection in which all energy is reflected only within the solid angle around the specular angle, measurement of the hemispherical reflectivity is possible. Substituting the measured hemispherical reflectivities in Eqs. (3–5) yields the optical constants and the thickness of the thin film. From this method, the measured thickness is 0.4 μm, and the measured thin film optical constants at $\lambda = 3.39$ μm are $n_2 = 1.92$, $\kappa_2 = 0.027$, and at $\lambda = 12.0$ μm they are $n_2 = 0.07$, $\kappa_2 = 1.02$. Comparisons of the measured data with the optical constants of pure aluminum oxide obtained by other investigators[3] were made. The measured values of n_2 are ~12 and 13% higher than the handbook values for $\lambda = 3.39$ and 12.0 μm, respectively, whereas a significantly larger value is noticed for the values of κ_2, which suggests the presence of some impurities or nonstoichiometric formation of the oxide layer in these samples.

The thickness of the thin film can also be measured by taking SEM pictures. A small piece of the sample is cut from the flat surface, and this sample is then mounted in epoxy with the exposed surface containing a cross section of the thin film. The cross section is polished in a series of polishing steps using abrasives of decreasing grit size down to 0.02 μm. It is then possible to take an SEM photograph of the cross section, as shown in Fig. 2. This cross section contains four layers. The top layer is epoxy; a thin gap of air exists between the oxide and epoxy. Under the oxide is aluminum. SEM pictures were taken at various locations across the thin film, and the thickness of the oxide was averaged. The measured value is 0.32 μm, which is only ~20% lower than the value estimated by

§Bi-Directional Reflectivity Data for Spectralon™ and Infragold™ samples, TMA, Inc., Bozeman, MT, 1994.

using hemispherical reflectivity measurements. This measured value is used in subsequent calculations.

Results and Discussion

In this section, the FTIR reflection measurements of the surface coated with aluminum-oxide composite are used to justify the accuracy of the thin film geometric optics approximation. This approximation is then used to demonstrate the influence of both the optical constants n_2 and κ_2 and the ratio of thin film thickness h/λ on reflection distribution. Table 1 shows optical constants and thickness used in each figure.

The reflection distribution of the random rough surface coated with aluminum-oxide composite is shown in Figs. 3 and 4 for incident directions of (θ_0, ϕ_0) = (30 deg, 0 deg), (35 deg, 0 deg), and (45 deg, 0 deg). All results are presented for a single reflection plane (0–180 deg) and scattering angles from −90 to 90 deg. Values at negative reflected angles are backscattered from positive incident angles. Figures 3 and 4 contain three sets of analytical predictions and one set of experimental findings. The rectangular dots are used to denote the FTIR measurements, whereas the lines with various thicknesses represent the analytical results based on the thin film geometric optics approximation with the same geometric parameters $\tau/\lambda = 20.2$ and $\sigma/\lambda = 7.20$ μm, but with different thin film properties n_2, κ_2, and h/λ. The first set of analytical results (——) are geometric optics predictions when the measured values of n_2, κ_2, and h/λ are used (see the preceding section and Table 1). The other two sets of results are the extreme variants of these predictions when $h/\lambda = 0$ (——) and $h/\lambda = \infty$ (▪ ▪ ▪). When $h/\lambda = 0$, there is no thin film and the surface is made entirely of pure aluminum. Similarly, when $h/\lambda = \infty$, the entire surface becomes pure aluminum-oxide composite. All analytical predictions have been averaged over the incident and reflected solid angles ($\Delta\Omega_0 = \Delta\Omega_s = \pm 3$ deg).

Figure 3 presents the results for an incident wavelength of 3.39 μm, where $\sigma/\tau = 0.36$ and $\sigma/\lambda = 7.20$. The geometric optics approximation predicts a diffuse reflection distribution for all three sets of input parameters. The energy spreads across most of the hemisphere. For the pure aluminum surface (no film), the bidirectional reflectivities from the geometric optics solutions significantly increase from −70 to 30 deg and reach a plateau for larger scattering angles. Integrating the bidirectional reflectivity over the entire hemisphere yields a hemispherical reflectivity of 1.00, which indicates that aluminum can be considered perfectly conducting. For the pure oxide surface, the magnitude of the reflection distribution is

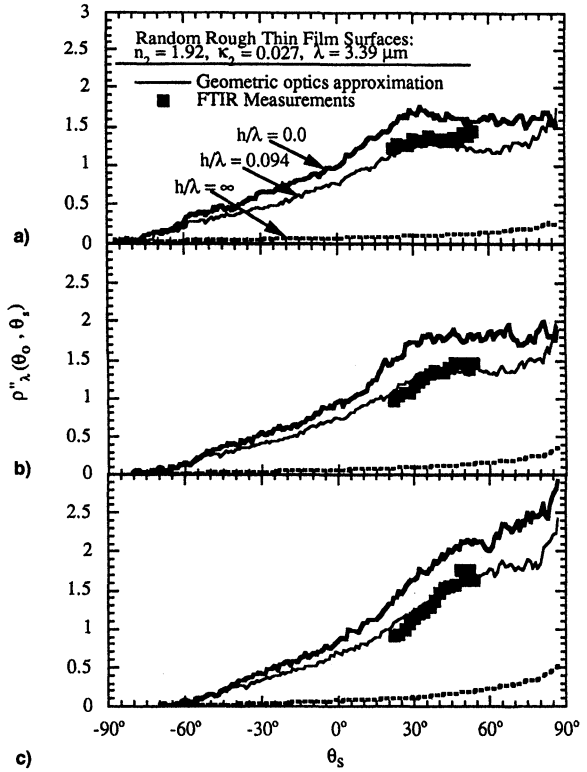

Fig. 3 Comparison of thin film geometric optics predictions with FTIR measurements for two-dimensional random rough surfaces coated with an absorbing thin film: $\sigma/\tau = 0.36$, $\sigma/\lambda = 7.20$, and $\phi_{0,s}$ = 0–180-deg plane. θ_0 = a) 30, b) 35, and c) 45 deg.

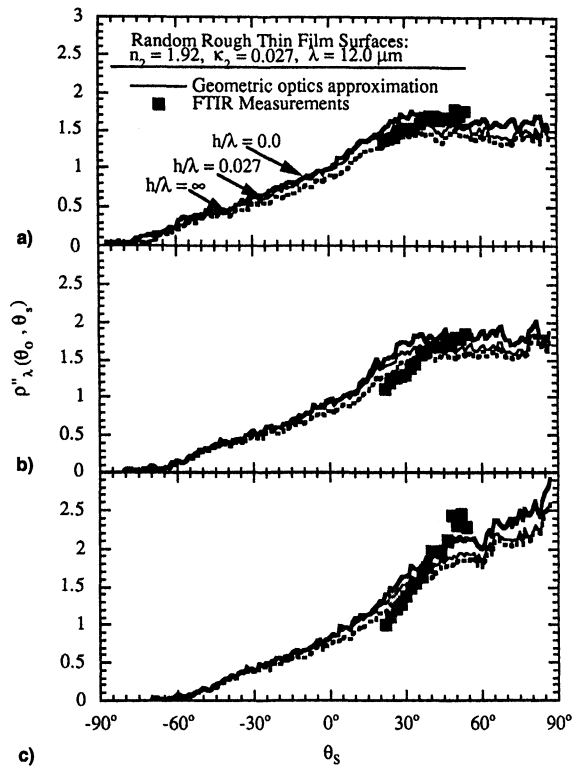

Fig. 4 Comparison of thin film geometric optics predictions with FTIR measurements for two-dimensional random rough surfaces coated with an absorbing thin film: $\sigma/\tau = 0.36$, $\sigma/\lambda = 2.09$, and $\phi_{0,s}$ = 0–180-deg plane. θ_0 = a) 30, b) 35, and c) 45 deg.

Table 1 Film thickness, incident angles, incident wavelengths, and optical constants for the calculations presented in Figs. 3–7

Figure	θ_0, deg	λ, μm	h/λ	n_2	κ_2	n_3	κ_3
3[a]	30, 35, 45	3.39	0.094	1.92	0.027	5.2	34.2
4[a]	30, 35, 45	12.0	0.027	0.07	1.02	33	103
5[b]	30	——	0.001–10.0	2.00	0.03	Perfectly conducting	——
6[b]	30	——	0.10	2.00	0.01–2.0	Perfectly conducting	——
7[b]	30	——	0.10	1.0–5.0	0.03	Perfectly conducting	——

[a]Predictions of the pure aluminum ($h/\lambda = \infty$) and pure oxide ($h/\lambda = 0.0$) surfaces are also presented in Figs. 3 and 4.
[b]Predictions of the pure perfectly conducting ($h/\lambda = \infty$) and pure absorbing film ($h/\lambda = 0.0$) surfaces are also presented in Figs. 5–7. For Figs. 6 and 7, the optical constants used for the predictions of the pure absorbing film are $n_2 = 2.00$ and $\kappa_2 = 0.03$.

significantly different from those of the pure aluminum and thin film surfaces. The bidirectional reflectivity distribution increases as the scattering angles increase, yet the values are much smaller than for aluminum. The hemispherical reflectivity is only 0.08. The effects of the thin film can be illustrated by comparing the results of the pure aluminum surface and the pure oxide surface. The thin film reflection distribution is entirely below that of the pure aluminum surface, and the thin film hemispherical reflectivity is only 0.78, indicating that a significant amount of incident energy is absorbed by the thin film. The experimental findings agree with the analytical predictions of the thin film case for all three incident angles, indicating the high accuracy of the thin film geometric optics approximation. Comparisons are also made at the incident wavelengths of 4.5 and 5.0 μm and similar results are observed.

Results for a relatively large incident wavelength (λ = 12.0 μm, where σ/τ = 0.36 and σ/λ = 2.1) are presented in Fig. 4. Similarly, FTIR measurements are presented along with the analytical predictions of the pure aluminum surface, the thin film surface, and the pure oxide surface. The measured optical constants and the thickness for λ = 12.0 μm are used (see the preceding section and Table 1). The geometric optics approximation predicts a diffuse reflection distribution, and no significant deviation in the reflection distribution is observed as the incident wavelength increases from 3.39 to 12.0 μm. However, for λ = 12.0 μm, the reflection distributions of the pure aluminum surface, the thin film surface, and the pure oxide surface are very similar in magnitude. They have a hemispherical reflectivity of 1.00, 0.94, and 0.87, respectively. Overall, the analytical predictions of the thin film case and the experimental findings are in good agreement. In addition, the ability of the geometric optics model to predict the experimental findings provides good confidence that the uniform film thickness assumption is valid.

When the thickness of the film is substantially larger than the incident wavelength, the effects of interference within the film can be neglected. The reflectance can be determined by tracking the fraction of incident energy multiply reflected within the film, and phase difference between reflected waves is not considered. The reflectivity is calculated based on the same multiple reflection mechanism; however, the total energy is found by simply adding the energy of each bundle leaving the film interface. Comparisons of the FTIR experimental findings with this energy method solution have been made for two incident wavelengths. For an incident wavelength of 3.39 μm, a deviation between the experimental findings and the energy method solution is observed, indicating that interference is important. The thin film hemispherical reflectivity calculated based on this energy method is only 0.78, which is ~10% lower than the hemispherical reflectivity when the interference is considered. For an incident wavelength of 12.0 μm, the energy method solutions agree with the FTIR experimental data. In this case, the oxide thin film is approximately perfectly conducting, and most of the energy is reflected from the top of the oxide surface layer without transmission. Thus, the interference is less important.

The thin film geometric optics approximation is used to study the reflection distribution for perfectly conducting surfaces that are coated with an absorbing thin film. The influence of film thickness and optical constants on reflection distribution are examined. Figures 5–7 present the bidirectional reflectivities from a random rough surface with σ/τ = 0.36 and σ/λ = 7.20. The incident angle is 30 deg and the incident wavelength is 3.39 μm.

The effects of film thickness are presented in Fig. 5, in which h/λ varies from 0.001 to 10. The results for the two extreme cases, pure perfectly conducting surface (h/λ = 0) and pure absorbing material (h/λ = ∞), are also presented for comparison. The optical constants of the absorbing material (n_2 = 2.00 and κ_2 = 0.03) are selected in this analytical calculation to approximate the values used in the previous FTIR experiment (n_2 = 1.92 and κ_2 = 0.027). As shown in Fig. 5, the entire reflection distribution of the case with h/λ = 0.001 corresponds closely with the case of the pure perfectly conducting surface, and these cases have a hemispherical reflectivity of 1.00 and 0.97. As h/λ increases to 0.1, the magnitude of the reflection distribution decreases, and hemispherical reflectivity is 0.83. This value is ~15% lower than cases with the pure perfectly conducting surface and with h/λ = 0.001. As the thickness further increases, the magnitude decreases until the film prediction aligns with the prediction of the pure absorbing material.

Figure 6 illustrates the influence of the imaginary part of the refractive index of the thin film κ_2 on the reflection distribution. Results of the two extreme cases are also presented. The values of the optical constants n_2 and thickness ratio h/λ are chosen to correspond to the experimental values, whereas κ_2 increases from 0.01 to 2.0. As shown in Fig. 6, unlike the thin film thickness, the influence of κ_2 is not monotonic. The entire

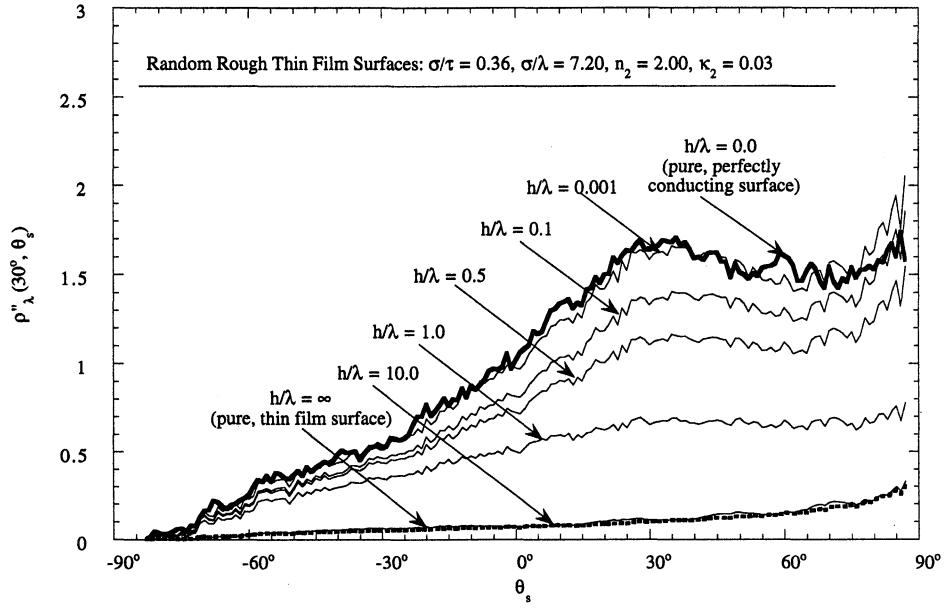

Fig. 5 Effect of the film thickness on the bidirectional reflectivity from random rough surfaces coated with an absorbing thin film as predicted by the thin film geometric optics approximation for θ_0 = 30 deg and ϕ_{0s} = 0–180 deg plane.

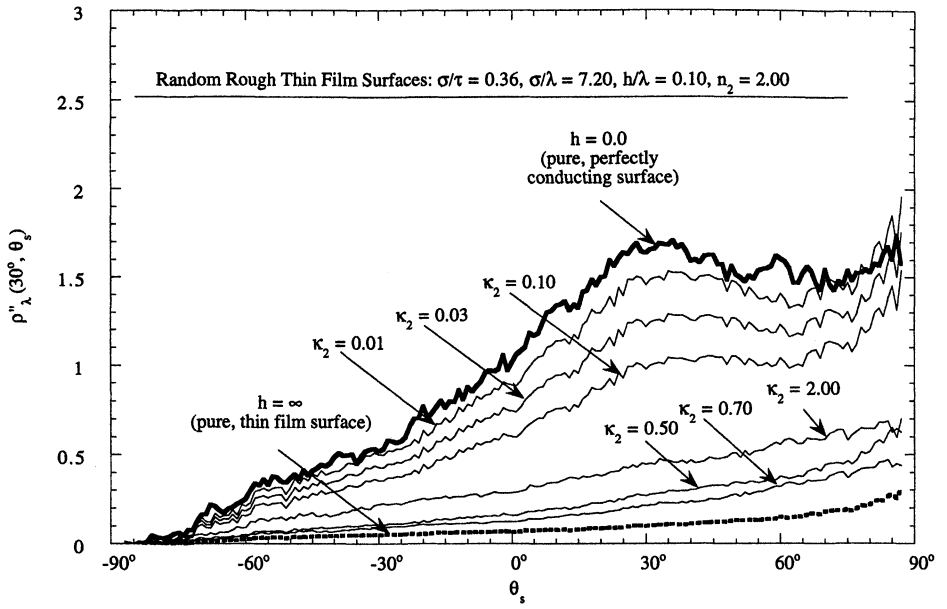

Fig. 6 Effect of film absorptive index on the bidirectional reflectivity from random rough surfaces coated with an absorbing thin film as predicted by the thin film geometric optics approximation for θ_0 = 30 deg and $\phi_{0,s}$ = 0–180-deg plane.

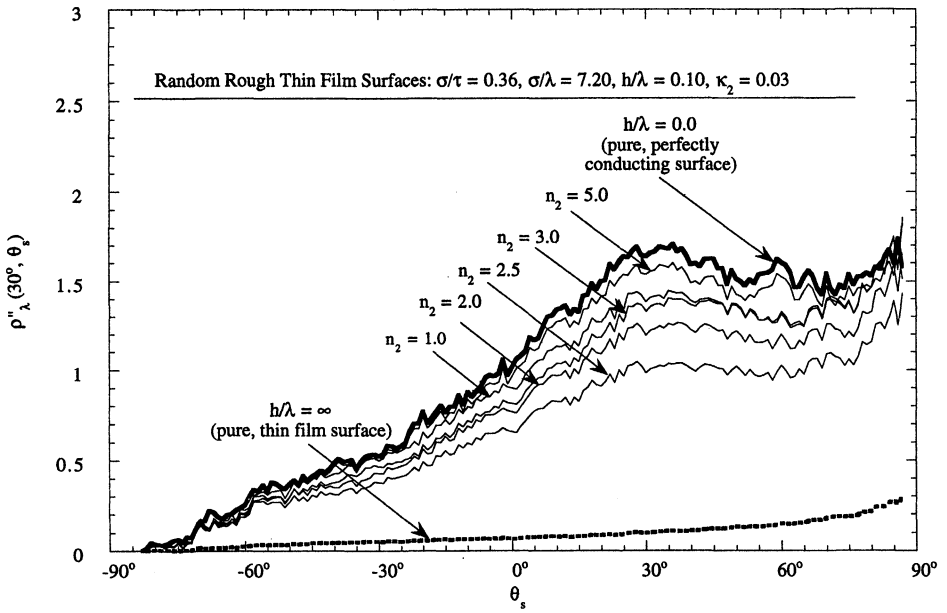

Fig. 7 Effect of film refractive index on the bidirectional reflectivity from random rough surfaces coated with an absorbing thin film as predicted by the thin film geometric optics approximation for θ_0 = 30 deg and $\phi_{0,s}$ = 0–180-deg plane.

reflection distribution shifts downward as κ_2 increases, and when κ_2 = 0.7, the hemispherical reflectivity reaches a minimum value of 0.17. A further increase of κ_2 results in an increase in the reflection distribution.

Similar predictions are presented in Fig. 7 for fixed h/λ and κ_2, and for n_2 between 1.0 and 5.0. The total internal reflection occurs when n_2 is less than n_1 = 1.0 and the hemispherical reflectivity is simply equal to unity. Thus, the cases with n_2 less than n_1 are not considered in the work. Similar to the imaginary part of the refractive index, the influence of n_2 is not monotonic. The magnitude of the entire reflection distribution decreases as n_2 increases from 1.0 to 2.0, corresponding to a decrease in hemispherical reflectivity from 0.90 to 0.83. The magnitude of reflection distribution reaches a minimum when n_2 is approximately equal to 2.5 and the hemispherical reflectivity is 0.67. As n_2 further increases from 2.5, an increase in the magnitude of reflection is observed until the film prediction is coincident with the pure perfectly conducting surface results.

To understand the contributions of the index of refraction as film reflection, Fig. 8 presents the hemispherical reflectivity of flat surfaces coated with an absorbing thin film. In the process of predicting the thin film geometric optics solutions for rough surfaces, each surface node is considered as a flat surface, and the hemispherical reflectivity calculated by Eq. (3) is used to account for the fraction of the reflected energy of each interaction. Thus, the hemispherical reflectivity of flat surfaces is the basic element of the thin film geometric optics approximation, and it can be used to study the nonmonotonic influence of optical constants on reflection distribution from rough thin film surfaces.

The incident angle is selected to be 30 deg in Fig. 8, and h/λ = 0.1. Two sets of results are included, and the optical constants of the thin film correspond to those used in Figs. 6

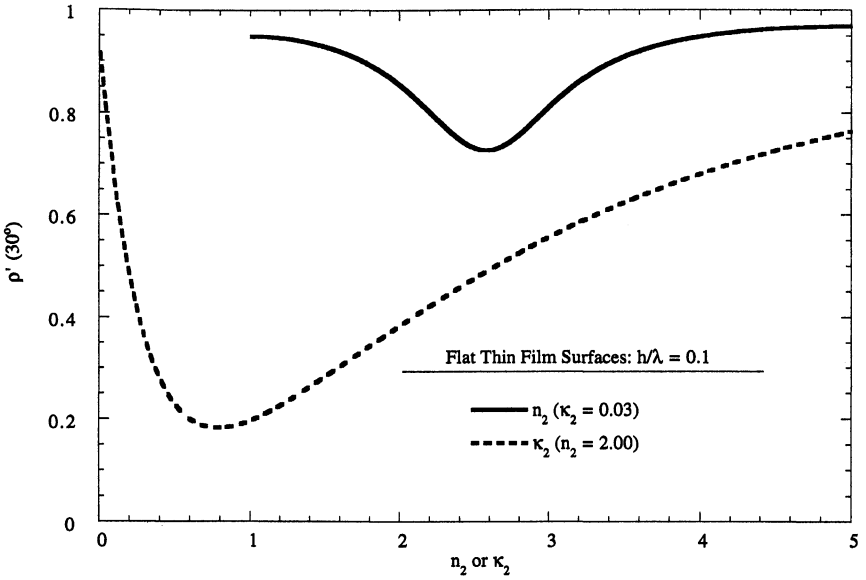

Fig. 8 Effects of optical constants on the hemispherical reflectivity of flat surfaces coated with an absorbing thin film as predicted by the thin film geometric optics approximation for θ_0 = 30 deg.

and 7. For the first set, $n_2 = 2.00$ and κ_2 is varied; and for the second set, n_2 is varied and $\kappa_2 = 0.03$. Results of n_2 less than n_1 are not reported. As κ_2 increases, the hemispherical reflectivity decreases and reaches a minimum value of 0.18 when $\kappa_2 = 0.7$. As κ_2 further increases, the hemispherical reflectivity gradually increases. For n_2, the hemispherical reflectivity exhibits the same trend and has a minimum value of 0.73 when $n_2 = 2.6$. This observation explains the nonmonotonic influence of optical constants on reflection distribution from rough thin film surfaces observed in the previous figures.

Conclusions

The geometric optics approximation is applied to predict reflection distribution from two-dimensional perfectly conducting random rough surfaces coated with an absorbing thin film. Comparison of the geometric optics predictions with the experimental findings is made for a random rough aluminum surface coated with a thin aluminum-oxide composite film. Results are compared at three incident angles and various wavelengths in the midinfrared region, and the predictions and experimental findings are in good agreement, indicating the accuracy of this model.

Using the thin film geometric optics approximation, the effects of the optical constants and the thickness of the thin film are also studied. As the thickness increases, the reflection distribution is reduced and the hemispherical reflectivity decreases. However, as the real and imaginary parts of the index of refraction increase, the reflection distribution initially shifts downward and reaches a minimum. The reflection distribution increases as the optical constants further increase.

Acknowledgments

This research was supported, in part, by the National Science Foundation, NSF CTS 95-31772; the University of Illinois Research Board; Pittsburgh Supercomputing Center; and the National Center for Supercomputing Applications. Surface profile measurements and the scanning electron microscopy were carried out in the Center for Microanalysis of Materials, University of Illinois. The authors thank Y. Yang for his assistance with the two-dimensional surface generation code.

References

[1]Maradudin, A. A., Michel, T., McGurn, A. R., and Mendez, E. R., "Enhanced Backscattering of Light from a Random Grating," *Annals of Physics*, Vol. 203, 1990, pp. 255–307.

[2]Dimenna, R. A., and Buckius, R. O., "Electromagnetic Theory Predictions of the Directional Scattering From Triangular Surfaces," *Journal of Heat Transfer*, Vol. 116, No. 3, 1994, pp. 639–645.

[3]Brewster, M. Q., *Thermal Radiative Transfer and Properties*, Wiley, New York, 1992.

[4]Dimenna, R. A., and Buckius, R. O., "Quantifying Specular Approximations for Angular Scattering from Perfectly Conducting Random Rough Surfaces," *Journal of Thermophysics and Heat Transfer*, Vol. 8, No. 3, 1994, pp. 393–399.

[5]Oren, M., and Nayar, S. K., "Generalization of Lambert's Reflectance Model," *Computer Graphics*, Annual Conference Series, 1994, pp. 239–246.

[6]Modest, M. F., *Radiative Heat Transfer*, McGraw–Hill, New York, 1993.

[7]Nieto-Vesperinas, M., and Sanchez-Gil, J. A., "Light Transmission from a Randomly Rough Dielectric Diffuser: Theoretical and Experimental Results," *Optics Letters*, Vol. 15, No. 22, 1990, pp. 1261–1263.

[8]Thorsos, E., "The Validity of the Kirchhoff Approximation for Rough Surface Scattering Using Gaussian Roughness Spectrum," *Journal of the Acoustical Society of America*, Vol. 83, No. 1, 1988, pp. 78–92.

[9]Chen, M. F., and Fung, A. K., "A Numerical Study of the Regions of Validity of the Kirchhoff and Small-Perturbation Rough Surface Scattering Models," *Radio Science*, Vol. 23, No. 2, 1988, pp. 163–170.

[10]McCammon, D. F., and McDaniel, S. T., "Surface Reflection: On the Convergence of a Series Solution to a Modified Helmholtz Integral Equation and the Validity of the Kirchhoff Approximation," *Journal of the Acoustical Society of America*, Vol. 79, No. 1, 1986, pp. 64–70.

[11]Liszka, E. G., and McCoy, J. J., "Scattering at a Rough Boundary—Extensions of the Kirchhoff Approximation," *Journal of the Acoustical Society of America*, Vol. 71, No. 5, 1982, pp. 1093–1100.

[12]Tang, K., Dimenna, R. A., and Buckius, R. O., "Regions of Validity of the Geometric Optics Approximation for Angular Scattering from Very Rough Surfaces," *International Journal of Heat and Mass Transfer*, Vol. 40, No. 1, 1997, pp. 49–59.

[13]Tang, K., and Buckius, R. O., "The Geometric Optics Approximation for Reflection from Two-Dimensional Random Rough Surfaces," *International Journal of Heat and Mass Transfer*, Vol. 41, No. 13, 1998, pp. 2037–2047.

[14]Wood, B. E., Bertrand, W. T., Bryson, R. J., Seiber, B. L., Falco, P. M., and Cull, R. A., "Surface Effects of Satellite Material Outgassing Products," *Journal of Thermophysics and Heat Transfer*, Vol. 2, No. 4, 1988, pp. 289–295.

[15]Wood, B. E., and Roux, J. A., "Infrared Optical Properties of Thin H_2O, NH_3, and CO_2 Cryofilms," *Journal of the Optical Society of America*, Vol. 72, No. 6, 1982, pp. 720–727.

[16]Nguyen, D. T., and Rustgi, M. L., "Diffraction of Plane Waves

from a Multilayered Film with a Grating Surface," *Journal of the Optical Society of America B*, Vol. 9, No. 10, 1992, pp. 1850–1856.
[17]Gunde, K. M., and Aleksandrov, B., "Infrared Optical Constants and Roughness Factor Functions Determination: The H_TH_RTR method," *Applied Optics*, Vol. 30, No. 22, 1991, pp. 3186–3196.
[18]Heavens, O. S., *Optical Properties of Thin Solid Films*, Dover, New York, 1965.
[19]Bennett, H. E., and Porteus, O. J., "Relation Between Surface Roughness and Specular Reflectance at Normal Incidence," *Journal of the Optical Society of America*, Vol. 51, No. 2, 1961, pp. 123–129.
[20]Tsuji, K., Yamada, T., Utaka, T., and Hirokawa, K., "The Effects of Surface Roughness on the Angle-Dependent Total-Reflection X-Ray Fluorescence of Ultrathin Film," *Journal of Applied Physics*, Vol. 78, No. 2, 1995, pp. 969–973.
[21]Pawlikowski, J. M., "Determination of the Absorption Coefficient of a Real Semiconductor Film: Application to ZnSe," *Thin Solid Films*, Vol. 125, No. 3, 4, 1985, pp. 213–220.
[22]Nagendra, C. L., and Thutupalli, G. K. M., "Optical Constants of Absorbing Materials: A New Approach," *Applied Optics*, Vol. 20, No. 15, 1981, pp. 2747–2753.
[23]Ford, J. N., Tang, K., and Buckius, R. O., "Fourier Transform Infrared System Measurements of the Bidirectional Reflectivity of Diffuse and Grooved Surfaces," *Journal of Heat Transfer*, Vol. 117, No. 4, 1995, pp. 955–962.
[24]Cohn, D. W., Tang, K., and Buckius, R. O., "Comparison of Theory and Experiments for Reflection of Microcontoured Surfaces," *International Journal of Heat and Mass Transfer*, Vol. 40, No. 13, 1997, pp. 3223–3235.
[25]Arnold, C. B., and Beard, J. L., "An ERIM Perspective on BRDF Measurement Technology," *Proceedings from the International Society for Optical Engineering*, Vol. 1165, 1989, pp. 112–135.